SOLUTION OF CORROSION PROBLEMS USING THE BOUNDARY ELEMENT METHOD

NOUF R. ALTALHI[1,2], DANIEL LESNIC[1] & STEPHEN D. GRIFFITHS[1]
[1]Department of Applied Mathematics, University of Leeds, UK
[2]Department of Mathematics, University of Taif, Saudi Arabia

ABSTRACT

In the practical setting of electrical impedance tomography, a current flux is injected through an electrode attached to the boundary and the boundary electrical potential is measured. This is numerically simulated by solving using the boundary element method (BEM) a direct problem for the Laplace equation with a nonlinear Butler–Volmer boundary condition over the boundary of a buried pipe that takes into account the principles of chemical corrosion. Our methodology is placed within the mathematical context of the Cauchy problem for the Laplace equation in a rectangular domain enclosing the corroded pipe whose boundary is inaccessible to prescribing any conditions on it. Given the Cauchy data, i.e. the specification of both the flux and potential, on an accessible portion of the boundary of the solution domain, the task is to determine the unknown potential and the flux on the inaccessible boundary of the pipe and the potential everywhere else inside the solution domain. This approach holds the promise of providing a non-invasive, accurate and effective means of detecting internal pipe corrosion, thus contributing significantly to maintaining safety standards in nuclear power plants. Since the inverse problem is ill-posed the resulting system of equations is ill-conditioned and the truncated singular value decomposition is employed in order to obtain stable and accurate numerical solutions. Other related inverse problems arising when modelling corrosion are also discussed.
Keywords: inverse problem, boundary elements, corrosion.

1 INTRODUCTION

Offshore structures such as sea platforms, bridges or ships made of metal are subjected to destructive corrosion attacks through electrochemical reactions with the air/water surroundings containing oxygen, or oxidizing agents, that affect their integrity [1]. Ensuring the integrity of piping systems is critical to management of nuclear power plants, where internal corrosion poses a significant risk to operational stability and safety. In order to understand the corrosion of a structure one needs to analyse the data on the electrical potential and the current density distribution over its boundary.

2 MATHEMATICAL FORMULATION

We consider an ion solution (electrolyte) occupying a bounded medium Ω within which the continuity equation

$$\nabla \cdot \underline{J} = 0 \quad \text{in} \quad \Omega \tag{1}$$

holds, where the current density vector $\underline{J}$ is related to the electrical potential ϕ through

$$\underline{J} = -\sigma \nabla \phi, \tag{2}$$

where σ is the conductivity of the medium, which may be isotropic or an-isotropic. In (1) we have assumed, for simplicity, that any source (or sink) generating current was absent. Introduction of (2) into (1) leads to the elliptic equation

$$-\nabla \cdot (\sigma \nabla \phi) = 0 \quad \text{in} \quad \Omega. \tag{3}$$

WIT Transactions on Engineering Sciences, Vol 136,
www.witpress.com, ISSN 1743-3533 (on-line)
doi:10.2495/BE470021

In this study, we consider only steady-state corrosion, with transient phenomena modelled by the parabolic heat equation being deferred to future study.

For simplicity, we assume that the electrolyte solution is homogeneous, i.e. $\sigma =$ constant, such that eqn (3) simplifies into the Laplace equation

$$\nabla^2 \phi = 0 \quad \text{in} \quad \Omega. \tag{4}$$

Nonlinear electrolytes with conductivity $\sigma = \sigma(\phi)$ dependent on the potential ϕ may also be considered and reduced to the Laplace equation via the Kirchhoff transformation $\psi = \int \sigma(\phi) d\phi$.

As for the boundary conditions associated to (4) we consider that a part of the boundary is electro-chemically active, where the oxidation-reduction reactions take place, while the remaining part is inactive, although we may inject a current flux on it. On the electro-chemically active metal-electrolyte boundary, owing to the polarization effect, the current flux is a nonlinear function of the potential difference $\eta_s := \phi - \phi_{eq}$ of the form [1],

$$J_e := \underline{J} \cdot \underline{n} = J_0 f(\phi - \phi_{eq}), \tag{5}$$

where $\underline{n}$ is the outward unit normal to the electrode's boundary, ϕ_{eq} is the equilibrium potential (also called the Nernst potential) of the electrode, J_0 is the exchange current density and f is a nonlinear polarization function.

If $|\eta_s|$ is small, then the nonlinear function in (5) is given by the Butler–Volmer equation [2],

$$f(\eta_s) = \exp(\beta\gamma\eta_s) - \exp(-(1-\beta)\gamma\eta_s), \tag{6}$$

where $\beta \in (0, 1)$ is a symmetry kinetic parameter called the transfer coefficient, $\gamma = F/(RT)$, where F is the Faraday's constant, R is the universal gas constant, T is the absolute temperature and the charge number of the dissolved or deposited species was taken to be equal to unity, for simplicity.

Based on (6), the boundary condition (5) can be written as [3],

$$-\sigma \frac{\partial \phi}{\partial n} = \underline{J} \cdot \underline{n} = J_0 \big(\exp(\beta\gamma\eta_s) - \exp(-(1-\beta)\gamma\eta_s) \big). \tag{7}$$

Defining

$$u := \gamma\eta_s = \frac{(\phi - \phi_{eq})F}{RT}, \tag{8}$$

we obtain from (4) and (7) that

$$\nabla^2 u = 0 \quad \text{in} \quad \Omega \tag{9}$$

and

$$\frac{\partial u}{\partial n} = \lambda \big(\exp(\beta u) - \exp(-(1-\beta)u) \big) \quad \text{on} \quad \Gamma_0, \tag{10}$$

where Γ_0 denotes the corroded boundary and

$$\lambda = -\frac{\gamma J_0}{\sigma} = -\frac{F J_0}{\sigma RT}. \tag{11}$$

www.witpress.com, ISSN 1743-3533 (on-line)

In general, $\lambda < 0$ on the active region where $|\eta_s|$ is small (at the anodic or cathodic surface) and $\lambda > 0$ in the transition region elsewhere [4].

The remaining part of the boundary $\partial\Omega\backslash\Gamma_0$ is assumed electrochemically inactive and we prescribe a Neumann condition

$$\frac{\partial u}{\partial n} = g \quad \text{on} \quad \partial\Omega\backslash\Gamma_0, \tag{12}$$

where g represents an imposed current flux.

3 MATHEMATICAL ANALYSIS

We write again the mathematical model of corrosion given by

$$\begin{cases} \nabla^2 u = 0 & \text{in } \Omega, \quad (13)\\ \dfrac{\partial u}{\partial n} = \lambda f(u) + g & \text{on } \Gamma_0, \quad (14)\\ \dfrac{\partial u}{\partial n} = g & \text{on } \partial\Omega \setminus \Gamma_0, \quad (15)\end{cases}$$

where possibly $g|_{\Gamma_0} = 0$ and

$$f(u) = \exp(\beta u) - \exp(-(1-\beta)u), \tag{16}$$

where $\beta \in (0, 1)$. Given $g \in L^2(\partial\Omega)$, the weak solution $u \in H^1(\Omega)$ of the problem (13)–(15) satisfies

$$\int_\Omega \nabla u \cdot \nabla v \, d\Omega = \int_{\Gamma_0} \lambda f(u)\, v \, d\Gamma_0 + \int_{\partial\Omega} g\, v\, ds, \quad \forall v \in H^1(\Omega). \tag{17}$$

Then the following theorem established in Vogelius and Xu [4] gives results on the unique solvability of the direct problem (13)–(15).

Theorem 3.1. *Given $g \in L^2(\partial\Omega)$, there exist $\lambda_0 > 0$ such that the solution to the problem (13)–(15) exists for any $\lambda \in (-\infty, \lambda_0)$. Moreover, for $\lambda \in (-\infty, 0]$ this solution is unique (except when $\lambda = 0$, which is unique up to a constant).*

When Ω is a disk in two-dimensions, the numerical investigations performed in Bryan and Vogelius [5] pointed out that there are infinitely many solutions to (13)–(16) for any $\lambda > 0$.

The Maclaurin series expansion

$$f(u) = \exp(\beta u) - \exp(-(1-\beta)u) \approx u + \frac{2\beta - 1}{2} u^2 + \ldots, \tag{18}$$

results in the linearized problem (near $|u| \ll 1$) given by

$$\begin{cases} \nabla^2 u = 0 & \text{in } \Omega, \quad (19)\\ \dfrac{\partial u}{\partial n} = \lambda u + g & \text{on } \Gamma_0, \quad (20)\\ \dfrac{\partial u}{\partial n} = g & \text{on } \partial\Omega \setminus \Gamma_0, \quad (21)\end{cases}$$

and the weak formulation (17) becomes

$$\int_{\Omega} \nabla u \cdot \nabla v \, d\Omega = \int_{\Gamma_0} \lambda u \, v \, d\Gamma_0 + \int_{\partial\Omega} g \, v \, ds, \quad \forall v \in H'(\Omega). \tag{22}$$

Then the unique solvability of the linear direct problem (19)–(21) holds for any real values of λ outside a countable set $\{\lambda_n\}_{n\geq 1}$ of positive integers ordered as $0 < \lambda_1 < \lambda_2 < \cdots$, see Vogelius and Xu [4].

4 THE BOUNDARY ELEMENT METHOD (BEM)

The BEM is well-suited for approaching numerically the direct problem (13)–(15) since the governing elliptic Laplace's equation (13) possesses an explicit fundamental solution given by

$$G(\underline{p}; \underline{p}') = \begin{cases} -\frac{1}{2\pi} \ln |\underline{p} - \underline{p}'| & \text{in two-dimensions} \\ \frac{1}{4\pi |\underline{p} - \underline{p}'|} & \text{in three-dimensions.} \end{cases} \tag{23}$$

Then classical application of Green's formula and imposition of the boundary conditions (14) and (15) results in the boundary integral representation of the solution as

$$\eta(\underline{p}) u(\underline{p}) = \int_{\Gamma_0} \lambda(\underline{p}') f(u(\underline{p}')) \, G(\underline{p}; \underline{p}') d\Gamma_0 + \int_{\partial\Omega} g(\underline{p}') \, G(\underline{p}; \underline{p}') ds \\ - \int_{\partial\Omega} u(\underline{p}') \frac{\partial G}{\partial n(\underline{p}')} (\underline{p}; \underline{p}') ds, \quad \underline{p} \in \overline{\Omega} = \Omega \cup \partial\Omega, \tag{24}$$

where $\eta(\underline{p}) = 1$ if $\underline{p} \in \Omega$ and $\eta(\underline{p}) = 0.5$ if $\underline{p}$ is on a smooth part of $\partial\Omega$. For simplicity, let us describe the BEM in two-dimensions only. Using a constant BEM approximation the function u is assumed to be piecewise constant and take the value at the midpoint (node) $\tilde{\underline{p}}_j = (\underline{p}_j + \underline{p}_{j-1})/2$ of each straight-line boundary element $S_j = [\underline{p}_{j-1}, \underline{p}_j]$ for $j = \overline{1, M}$, discretising in an anti-clockwise sense the boundary $\partial\Omega$ where M denotes the number of boundary elements and $\underline{p}_M = \underline{p}_0$ by convention, namely,

$$u(\underline{p}') = u(\tilde{\underline{p}}_j) =: u_j, \quad \forall \underline{p}' \in S_j, \quad j = \overline{1, M}. \tag{25}$$

We also approximate

$$g(\underline{p}') = g(\tilde{\underline{p}}_j) =: g_j, \quad \forall \underline{p}' \in S_j, \quad j = \overline{1, M}, \tag{26}$$

$$\lambda(\underline{p}') = \lambda(\tilde{\underline{p}}_j) =: \lambda_j, \quad \forall \underline{p}' \in S_j, \quad j = \overline{1, N}. \tag{27}$$

Assume that Γ_0 is discretised by the first N boundary elements. Then, based on (25)–(27), eqn (24) yields the BEM approximation

$$\eta(\underline{p}) u(\underline{p}) = \sum_{j=1}^{N} \lambda_j f(u_j) \int_{S_j} G(\underline{p}; \underline{p}') dS_j + \sum_{j=1}^{M} g_j \int_{S_j} G(\underline{p}; \underline{p}') dS_j \\ - \sum_{j=1}^{M} u_j \int_{S_j} \frac{\partial G}{\partial n(\underline{p}')} (\underline{p}; \underline{p}') dS_j, \quad \underline{p} \in \overline{\Omega}. \tag{28}$$

www.witpress.com, ISSN 1743-3533 (on-line)

Denoting by

$$A_j(\underline{p}) = \int_{S_j} G(\underline{p};\underline{p}')dS_j, \quad B_j(\underline{p}) = \int_{S_j} \frac{\partial G}{\partial n}(\underline{p};\underline{p}')dS_j, \quad j=\overline{1,M}, \tag{29}$$

which can be evaluated analytically based on the geometry of the triangle $\Delta\, \underline{p}\, \underline{p}_{j-1}\, \underline{p}_j$, see e.g. Jaswon and Symm [6], the boundary integral equation (28) can be rewritten as

$$\eta(\underline{p})u(\underline{p}) = \sum_{j=1}^{N} A_j(\underline{p})\lambda_j f(\underline{u}_j) + \sum_{j=1}^{M} A_j(\underline{p})g_j - \sum_{j=1}^{M} B_j(\underline{p})u_j, \qquad \underline{p} \in \overline{\Omega}, \tag{30}$$

where we are assuming that Γ_0 is discretised by the first N boundary elements.

Collocating (30) at the boundary nodes $\left(\underline{\tilde{p}}_i\right)_{i=\overline{1,M}}$ results in the following system of M nonlinear equations with M unknowns $(u_j)_{j=\overline{1,M}}$:

$$\sum_{j=1}^{N} (A_{ij}\lambda_j f(u_j) + B_{ij}u_j) + \sum_{j=N+1}^{M} B_{ij}u_j = -\sum_{j=1}^{M} A_{ij}g_j \quad \text{for} \quad i=\overline{1,M}, \tag{31}$$

where

$$A_{ij} = A_j(\underline{\tilde{p}}_i) \ \text{ and } \ B_{ij} = -B_j(\underline{\tilde{p}}_i) - \frac{1}{2}\delta_{ij},$$

and δ_{ij} is the Kronecker-delta tensor.

For the linear boundary condition $\partial_n u = \lambda u$ on Γ_0, the system (31) becomes linear and is given by

$$\sum_{j=1}^{N}(A_{ij}\lambda_j + B_{ij})u_j + \sum_{j=N+1}^{M} B_{ij}u_j = -\sum_{j=1}^{M} A_{ij}g_j \quad \text{for} \quad i=\overline{1,M}. \tag{32}$$

4.1 Numerical discretisation

For the two-dimensional bounded geometry of Ω, we consider a doubly-connected annular domain consisting of an infinitely-long cylindrical circular buried pipe, which is subjected to a corrosion attack. Due to the symmetry of the problem, we can consider only a quadrant of the geometry, as pictured, along with the relevant boundary conditions, in Fig. 1. The boundary Γ_0 is the first quarter of the unit circle, whilst $\Gamma = \partial\Omega \setminus \Gamma_0$ is the remaining part consisting of the horizontal and vertical portions Γ_i for $i=\overline{1,4}$. Then, due to symmetry, clearly $g=0$ on $\Gamma_1 \cup \Gamma_4$. Also, by assuming that the top wall is adiabatic we have that $g=0$ on Γ_3. On the vertical wall Γ_2, we impose a current flux over an electrode of length 2ϵ centered at $(2, \frac{1}{3})$ which is drawn out over another electrode of length 2ϵ centered at $(2, \frac{2}{3})$, where $\epsilon > 0$ is a small number, typically $\epsilon = 0.1$. Therefore, on Γ_2, the current flux is given by

$$g(2,y) = \begin{cases} 0 & \text{if} \quad 0 \le y < \frac{1}{3} - \epsilon, \\ \frac{1}{2\epsilon} & \text{if} \quad \frac{1}{3} - \epsilon \le y \le \frac{1}{3} + \epsilon, \\ 0 & \text{if} \quad \frac{1}{3} + \epsilon < y < \frac{2}{3} - \epsilon, \\ -\frac{1}{2\epsilon} & \text{if} \quad \frac{2}{3} - \epsilon \le y \le \frac{2}{3} + \epsilon, \\ 0 & \text{if} \quad \frac{2}{3} + \epsilon < y \le 2. \end{cases} \tag{33}$$

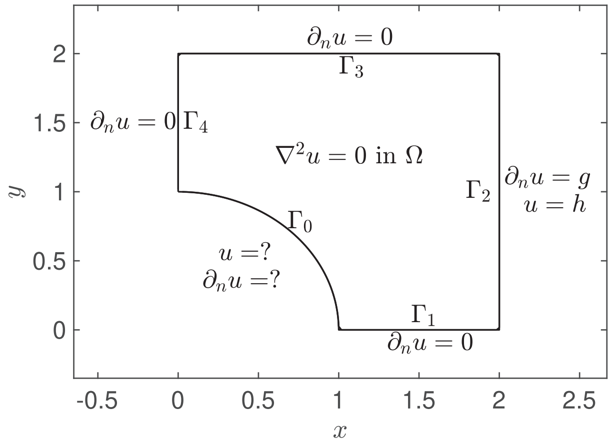

Figure 1: Cauchy inverse problem formulation.

We also take $g = 0$ on Γ_0 in which case the boundary condition (20) becomes

$$\frac{\partial u}{\partial n} = \lambda f(u) \quad \text{on} \quad \Gamma_0, \tag{34}$$

where $f(u) = u$ in the linear case and $f(u) = 2\sinh(u/2)$ in the nonlinear case.

The boundary $\partial\Omega$ is uniformly discretized in an anti-clockwise direction starting from the point (0,1), with each of the boundaries Γ_0, Γ_1, and Γ_4 using N boundary elements, and Γ_2 and Γ_3 each using $2N$ boundary elements. This way the total number of boundary elements discretising $\partial\Omega$ is $M = 7N$.

The numerical solution of the direct problem given by eqns (13)–(15) is obtained using the BEM based on solving the system of eqns (31) (or (32)). We have also applied the method of fundamental solutions (MFS), Karageorghis and Lesnic [7], to solving the direct problem (13)–(15) and we have obtained similar results to those obtained by the BEM, re-ensuring that the numerical BEM solution is accurate.

Next, the data $u\,|_{\Gamma_2} =: h$ is employed as an extra piece of information to solve the Cauchy inverse problem depicted in Fig. 1, and given by

$$\begin{cases} \nabla^2 u = 0 & \text{in } \Omega, & (35) \\ \dfrac{\partial u}{\partial n} = g & \text{on } \partial\Omega \setminus \Gamma_0, & (36) \\ u = h & \text{on } \Gamma_2. & (37) \end{cases}$$

This inverse problem arises due to the inaccessibility of measuring along the corroded boundary Γ_0 of the buried pipe. Note that the inverse problem (35)–(37) is linear and ill-posed (the solution is unique but it does not depend continuously on the input data h), whilst the direct problem (13)–(15) is non-linear (through the boundary condition (14) if $f(u)$ is nonlinear function of u) and well-posed (under the conditions stated in Theorem 3.1).

The BEM numerical discretisation of the inverse problem (35)–(37) results in the following overdetermined system of M linear equations in $(M-N)$ unknowns:

$$\sum_{j=1}^{N} A_{ij}u'_j + \sum_{j=1}^{2N} B_{ij}u_j + \sum_{j=4N+1}^{M} B_{ij}u_j$$
$$= - \sum_{j=N+1}^{M} A_{ij}g_j - \sum_{j=2N+1}^{4N} B_{ij}h_j \quad \text{for } i=\overline{1,M}, \tag{38}$$

where, based on the BEM with constant elements,

$$u'_j := \frac{\partial u}{\partial n}(\underline{\tilde{p}}_j) = \frac{\partial u}{\partial n}(\underline{p}'), \quad \forall \underline{p}' \in S_j, \quad j=\overline{1,N},$$
$$h_j := h(\underline{\tilde{p}}_j) = h(\underline{p}'), \quad \forall \underline{p}' \in S_j, \quad j=\overline{2N+1,4N}.$$

In a matrix form, the system of eqns (38) can be written as

$$K\underline{X} = \underline{b}, \tag{39}$$

where

$$K_{ij} = \begin{cases} A_{ij} & \text{for } j=\overline{1,N}, \\ B_{ij} & \text{for } j=\overline{1,2N} \text{ and } j=\overline{4N+1,M}, \end{cases} \quad \text{and } i=\overline{1,M},$$
$$\underline{X} = \left((u'_j)_{j=\overline{1,N}}, (u_j)_{j=\overline{1,2N}}, (u_j)_{j=\overline{4N+1,M}}\right)^{\mathrm{T}},$$
$$b_i = - \sum_{j=N+1}^{M} A_{ij}g_j - \sum_{j=2N+1}^{4N} B_{ij}h_j \quad \text{for } i=\overline{1,M}.$$

5 NUMERICAL RESULTS AND DISCUSSION

For simplicity, we take $\lambda = 1$ and illustrate the numerical results obtained for the linearised boundary condition $\partial_n u = \lambda u$ on Γ_0. Although not illustrated, it is reported that similar results have been obtained for the nonlinear boundary condition $\partial_n u = 2\lambda \sinh(u/2)$ on Γ_0, due to the approximation (18) being valid in a small neighbourhood of the origin (for the direct problem with the data g given by (33) on Γ_0 and zero elsewhere, we have obtained that the range of $u|_{\Gamma_0}$ is within $(-0.2, 0.2)$, see e.g. Fig. 3(a)).

We first solved the direct problem based on the BEM system of eqns (38) with $N = 30$ to obtain the data $h = u|_{\Gamma_2}$ to be used in solving the inverse problem based on the BEM system of eqns (39). Since the Cauchy problem (35)–(37) is ill-posed, the resulting system of eqns (39) is ill-conditioned. This is reflected in the behaviour of the normalised singular values of the matrix K (of dimension $M \times (M-N) = 210 \times 180$) displayed in Fig. 2. The normalised singular values start off at a maximum value of 1 (since they are normalized by the largest singular value) and exhibit a steep decline, eventually spanning several orders of magnitude after about 150 singular values. This characteristic decay pattern is indicative of the presence of both significant and negligible components in the data structure. It suggests that the matrix from which these singular values are derived may be well-conditioned in the higher index range but becomes increasingly ill-conditioned as the index increases. Such a plot is crucial in the context of regularization, where one may truncate the spectrum to mitigate the effects of noise amplification, retaining only the most significant singular values for obtaining a stable solution [8].

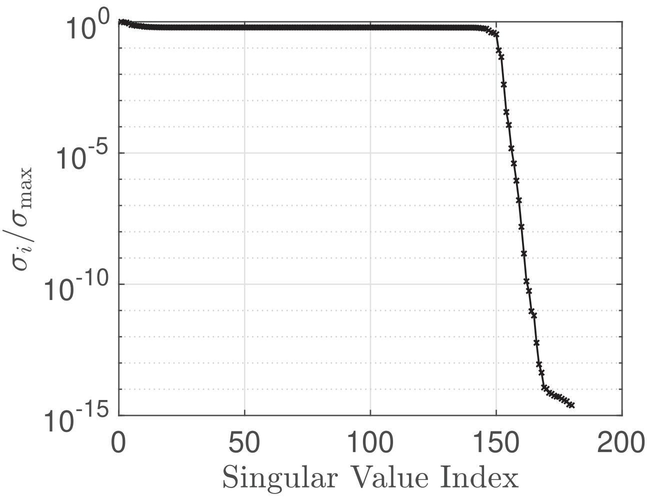

Figure 2: Normalized singular values of the matrix K.

Figs 3(a) and 3(b) present the numerical solutions for u and $\partial_n u$ on Γ_0 obtained using the untruncated singular value decomposition method (SVD) for solving the system of eqns (39), whilst Figs 3(c) and 3(d) present the numerical solutions obtained using the truncated singular value decomposition method (TSVD) taking into account only the first 166 singular values. Employing the SVD method produced an accurate numerical solution for u on Γ_0, as shown in Fig. 3(a). However, the numerical solution for the normal derivative $\frac{\partial u}{\partial n}$ on Γ_0 shown in Fig. 3(b) manifests expected instabilities. Discarding the very low singular values results in stable approximations illustrated in Fig. 3(d) by truncating the SVD expansion at 166 singular values.

To investigate further the stability of the TSVD, we invert noisy boundary temperature measured data on Γ_2, numerically simulated as

$$h_j^{noisy} = h_j(1 + p\rho_j), \quad j = \overline{(2N+1), 4N}, \tag{40}$$

where p represents the percentage of multiplicative noise and $(\rho_j)_{j=\overline{(2N+1),4N}}$ are random variables drawn from a uniform distribution in $[-1, 1]$. Fig. 4 presents the numerical results obtained without and with truncation in the SVD, when $p = 1\%$ noisy data (40) are inverted. From this figure the role of appropriate truncation acting as a stable regularization can be observed. The choice of the truncation number in the TSVD depends on the amount of noise with which the data h is contaminated by (40) and can be chosen according to the discrepancy principle or the L-curve method [9].

6 OTHER INVERSE PROBLEMS ARISING IN CORROSION

Other inverse problems related to possible unknown quantities present in eqn (14) can be formulated [10], [11], as follows.

6.1 Determination of the coefficient of corrosion

Another inverse problem arising in corrosion engineering requires determining the coefficient of corrosion λ on Γ_0, see e.g. [12], [13], in case it is unknown in the boundary condition

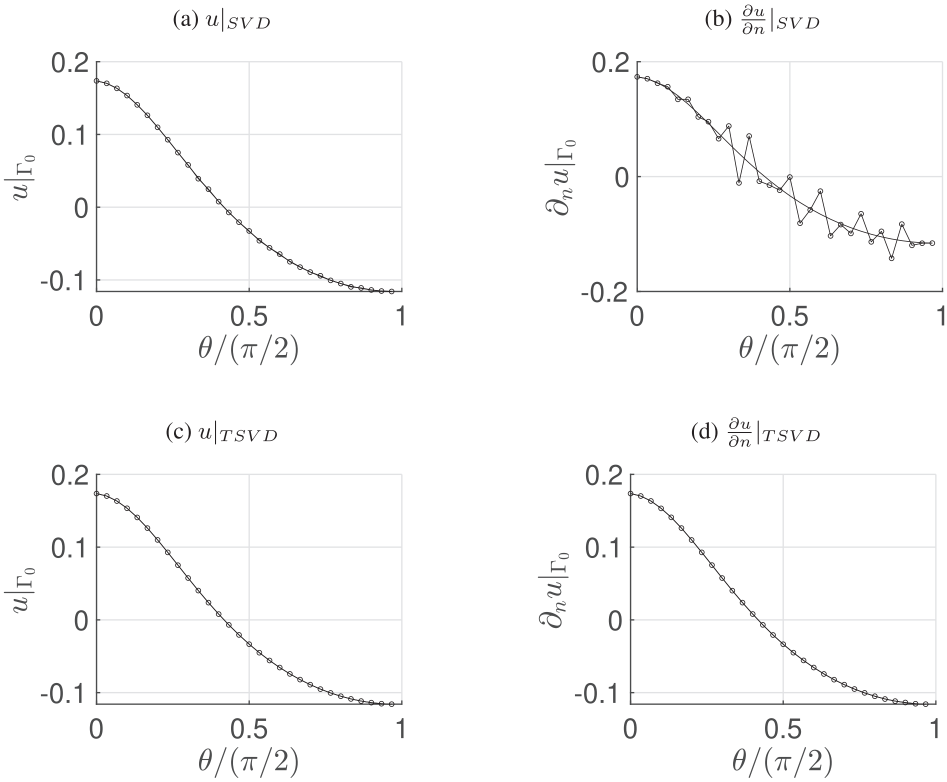

Figure 3: The numerical BEM solutions for u and the normal derivative $\frac{\partial u}{\partial n}$ on Γ_0 of the inverse problem $(-\circ-)$ with noiseless data obtained using: (a,b) the untruncated SVD; and (c,d) the TSVD truncated at 166 singular values, in comparison with the BEM solutions of the direct problem (——).

(14). In our setup, once the values of u and $\partial_n u$ have been accurately determined on Γ_0, the coefficient of corrosion λ can simply be estimated from (14) as

$$\lambda_j = \frac{u'_j - g_j}{f(u_j)}, \quad j = \overline{1, N}, \tag{41}$$

with the convention that the l'Hopital rule may need to be employed if a $0/0$ non-determination occurs at isolated points on Γ_0.

For the example considered in the previous section, for noiseless data, i.e. $p = 0$ in (40), employing eqn (41) yields a very accurate estimation of the exact coefficient $\lambda_{exact}(\theta) \equiv 1$ for $\theta \in [0, \pi/2]$, simply dividing the numerical solution of Fig. 3(d) by that of Fig. 3(c). No inaccuracies were obtained close to the end points $\theta = 0$ or $\theta = \pi/2$ of the circular arc Γ_0 nor close to the point $\theta \approx \frac{\pi}{2} \times 0.4$, where both u and $\partial_n u$ vanish. However, in case of noisy data, by dividing the numerical solution of Fig. 4(d) by that of Fig. 4(c) results in a highly oscillatory and unbounded retrieval of the coefficient of corrosion. In this case, in order to restore stability, nonlinear iterative regularization needs to be employed in a future work.

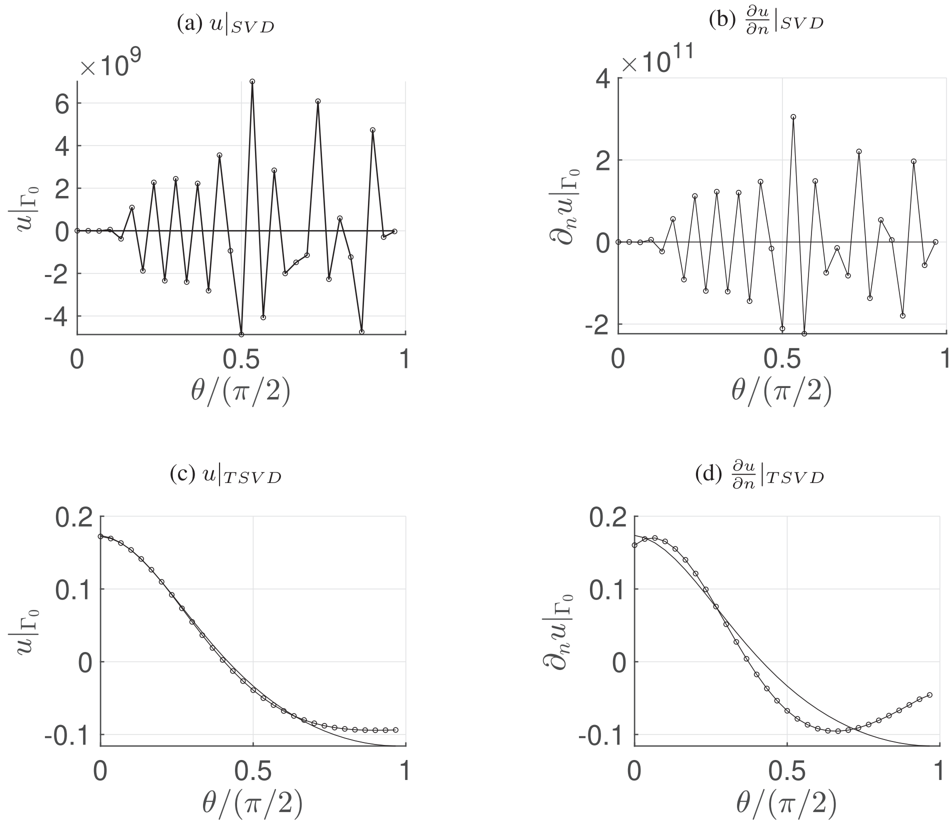

Figure 4: The numerical BEM solutions for u and the normal derivative $\frac{\partial u}{\partial n}$ on Γ_0 of the inverse problem $(-\circ-)$ with $p = 1\%$ noisy data obtained using: (a,b) the untruncated SVD; and (c,d) the TSVD truncated at 152 singular values, in comparison with the BEM solutions of the direct problem (——).

6.2 Determination of the law of corrosion

Another inverse problem relates to the identification of the law of corrosion $f(u)$ present in the boundary condition (14), see e.g. [14], [15]. In this case, one can try to plot u versus $\partial_n u$ from Figs 3(c) and 3(d), in case of noiseless data, or from Figs 4(c) and 4(d), in case of noisy data, and try to infer from the graph obtained the behaviour of the function $f(u)$, as a function of u. Again, as before, this simple graphical method may work in case of error-free data, but it becomes less effective in case of noisy data. In order to overcome this situation, regularization by discretisation [16] could be employed.

6.3 Determination of the corroded boundary

In the physical case that the corroded boundary Γ_0 is unknown, the single measurement (37) of u on Γ_2 is, in general, not sufficient to determine Γ_0, see Cakoni and Kress [17]. However, two linearly independent pairs of Cauchy data $(u, \partial_n u) = (g_i, h_i)$ for $i = 1, 2$ are sufficient to determine not only the corroded boundary Γ_0 but also the coefficient of corrosion λ, in the case where the law of corrosion is linear [18].

7 CONCLUSIONS

This paper has presented a thorough investigation of the BEM for solving inverse problems under both noise-free and noisy input data for linear and non-linear boundary-condition models of non-destructive pipe corrosion testing. The numerically-obtained results have demonstrated that the TSVD provides a reliable stable method of solution for recovering the unknown data on the corroded boundary. The findings emphasize the necessity of methodological rigor and the need for robust computational strategies adaptable to data imperfections.

ACKNOWLEDGEMENTS

In deep appreciation for the generous sponsorship provided by Taif University, N.R. Altalhi extends heartfelt gratitude. No data are associated with this article.

REFERENCES

[1] Fontana, M.G. & Greene, N.D., *Corrosion Engineering*, McGraw-Hill Book Company, 1978.
[2] Bockris, J.O. & Reddy, A.K., *Modern Electrochemistry*, Springer Science and Business Media, 1974.
[3] Zamani, N., Porter, J. & Mufti, A., A survey of computational efforts in the field of corrosion engineering. *International Journal for Numerical Methods in Engineering*, **23**, pp. 1295–1311, 1986.
[4] Vogelius, M. & Xu, J.M., A nonlinear elliptic boundary value problem related to corrosion modeling. *Quarterly of Applied Mathematics*, **56**, pp. 479–505, 1998.
[5] Bryan, K. & Vogelius, M., Singular solutions to a nonlinear elliptic boundary value problem originating from corrosion modeling. *Quarterly of Applied Mathematics*, **60**, pp. 675–694, 2002.
[6] Jaswon, M.A. & Symm, G.T., *Integral Equation Methods in Potential Theory and Elastostatics*, Academic Press, 1977.
[7] Karageorghis, A. & Lesnic, D., The method of fundamental solutions for steady-state heat conduction in nonlinear materials. *Communications in Computational Physics*, **4**, pp. 911–928, 2008.
[8] Hansen, P.C., *Rank Deficient and Discrete Ill-Posed Problems: Numerical Aspects of Linear Inversion*, SIAM, 1998.
[9] Hansen, P.C., Analysis of discrete ill-posed problems by means of the L-curve. *SIAM Review*, **34**, pp. 561–580, 1992.
[10] Sincich, E., Stability and reconstruction for inverse corrosion problems. *Journal of Inverse and Ill-Posed Problems*, **17**, pp. 783–794, 2009.
[11] Rundell, W., Recovering an obstacle and its impedance from Cauchy data. *Inverse Problems*, **24**, pp. 783–794, 045003, 2008.
[12] Choulli, M., An inverse problem in corrosion detection: Stability estimates. *Journal of Inverse and Ill-Posed Problems*, **26**, pp. 453–457, 2018.
[13] Jin, B. & Jun, Z., Numerical estimation of the Robin coefficient in a stationary diffusion equation. *IMA Journal of Numerical Analysis*, **30**, pp. 677–701, 2010.

[14] Fasino, D. & Inglese, G., Recovering unknown terms in a nonlinear boundary condition for Laplace's equation. *IMA Journal of Applied Mathematics*, **71**, pp. 832–852, 2006.
[15] Fasino, D. & Inglese, G., Recovering nonlinear terms in an inverse boundary value problem for Laplace's equation: A stability estimate. *Journal of Computational and Applied Mathematics*, **198**, pp. 460–470, 2007.
[16] Cao, H., Pereverzev, S.V. & Sincich, E., Natural linearization for corrosion identification. *Journal of Physics: Conference Series*, **135**, 012027, 2008.
[17] Cakoni, F. & Kress, R., Integral equations for inverse problems in corrosion detection from partial Cauchy data. *Inverse Problems and Imaging*, **1**, pp. 229–245, 2007.
[18] Bacchelli, V., Uniqueness for the determination of unknown boundary and impedance with the homogeneous Robin condition. *Inverse Problems*, **25**, 015004, 2009.